

Coordinate Independent Forms of the Compressible Potential Flow Equations

Tony Saad,^{*} Brian A. Maicke[†] and Joseph Majdalani[‡]
University of Tennessee Space Institute, Tullahoma, TN 37388

The compressible motion of gases has long been connected with high energy yield devices such as combustors, jet engines, turbines, and rocket motors. Most available formulations for this high speed gaseous environment lead to coupled nonlinear PDEs. While their integration requires the use of numerical methods, their stability and convergence remain conditional on the stiffness of the system. In seeking reduced-order models, it has become customary to introduce specific assumptions that simplify the problem's complexity without sacrificing its fundamental physical attributes. Examples include the variety of low-Mach number models for subsonic combustion and atmospheric flows, or the high-Mach number schemes used in the treatment of hypersonic motions. The ensuing approximations constitute limiting process expressions of the original equations and are often accompanied by their own stability and convergence criteria. Another reduction in complexity may be accomplished by relaxing certain physical constraints or implementing simplifying assumptions that correspond, if the situation permits, to inviscid, adiabatic, and non-reactive models. A classic example is the study of acoustic instability in solid rocket motors where some analyses consider the flow to be irrotational. For the variety of reasons mentioned, we consider in this work the limiting potential case of the compressible gaseous motion not only in propulsion devices, such as rockets and other confined thrust chambers, but also in external aerodynamic flows as well. In this spirit, we derive the equations of motion for a steady, irrotational, compressible fluid in coordinate-independent vector form. We accomplish this using two approaches, one based on the velocity potential, and the other using the streamfunction formulation. In both instances, the spatial dependence of the speed of sound is eliminated in favor of its stagnation value. This key aspect of the present framework enables us to systematically apply the Rayleigh-Janzen asymptotic technique to explicitly solve the compressible potential equations in the low-Mach number limit. While the procedure is rather straightforward with the velocity potential, auxiliary relations are required when using the streamfunction approach. By way of example, the two formulations developed here are implemented to the extent of producing analytical approximations for two geometric settings associated with the irrotational compressible flowfields in planar and cylindrical rocket motors.

Nomenclature

\mathbf{u}	velocity field
x	spatial coordinate
c	speed of sound
M	Mach number
p	pressure
<i>Greek</i>	
ϕ	velocity potential, $\mathbf{u} = \nabla\phi$
ψ	streamfunction
ρ	density

Subscripts

* dimensional variable

Superscripts

0 stagnation condition
 ∞ free stream condition

^{*}Presently Postdoctoral Fellow, Institute for Clean and Secure Energy, University of Utah. Member AIAA.

[†]Graduate Research Assistant, Mechanical, Aerospace, and Biomedical Engineering Department. Member AIAA.

[‡]H. H. Arnold Chair of Excellence in Advanced Propulsion and Professor, Mechanical, Aerospace, and Biomedical Engineering Department. Associate Fellow AIAA. Fellow ASME.

I. Introduction

THE compressible high speed motion of gases has long been a challenging area of investigation in fluid dynamics. A wealth of new and often unexpected phenomena are frequently reported under compressible fluid conditions, thus making their mathematical treatment crucial for a meaningful physical description. Examples include numerous industrial systems and almost all high energy yield devices such as combustors, rocket motors, jet engines, gas turbines, and internal combustion engines, where flowfields undergo significant levels of compression and expansion.¹

The analysis of high speed gases is not only relevant to internal flows, but also to unbounded motions that arise in external aerodynamics. In this context, adequate understanding of the shock wave/structure interactions has been shown to be essential for the proper design of airborne vehicles.² The recent thrust in modeling hypersonic flows with their underpinning challenges such as heating, molecular dissociation and supersonic combustion³ constitutes another such example where fluid compression can have substantial ramifications on vehicle design,⁴ mission profile, and flight envelope. Unquestionably, the need for improved modeling capabilities continues to grow.^{5,6}

In its simplest form, the key characteristic of a compressible fluid may be represented by the relative speeds of convective and acoustic propagation of disturbances. Their actual ratio constitutes the well known Mach number that gauges the relative intensity of compressibility forces. When the acoustic waves are at least one order of magnitude faster than their convective counterparts ($M < 0.3$), one may safely dismiss the effect of compressibility; otherwise, its inclusion is often required.

The basic description of high speed gaseous motion is represented by a nonlinear set of partial differential equations that may be considered as a generalization of the Navier-Stokes equations. These equations require a variety of closure models to completely determine the thermodynamic state of the system at hand. In the early development of external aerodynamics, the favored methods were based on reduced-order models, such as one-dimensional formulations, to facilitate the integrability of the compressible flow equations.⁷ With simulation science becoming a mature field, less modeling is now required as numerical methods have markedly evolved and are now fully capable of handling the attendant equations.⁸ Nonetheless, with the advent of improved numerical modeling capabilities, a variety of convergence, stiffness and stability issues emerge as well.^{9,10} Today, reduced-order formulations and limiting process approximations continue to receive favor in many research circles.¹¹⁻¹³ One such example corresponds to the low-Mach number limit that has been successfully used to model acoustic waves,¹⁴ reactive gases,⁹ solid rocket motor (SRM) flowfields,¹⁵⁻¹⁸ and atmospheric air^{19,20} in the subsonic regime.

Another reduction in complexity is accomplished by relaxing overly constraining features of the problem. Traditionally used assumptions lead to inviscid, adiabatic, and non-reactive models. These are useful when the solution being sought is to be employed as a first approximation. For example, the model may provide the outer solution of an elaborate problem that involves, as the case may be, both outer and inner flow regions. A classic example is the study of acoustic instability in solid rocket motors where the outer mean flow is sometimes assumed to be irrotational in the farfield²¹⁻²³ to the extent that boundary layers may be dealt with separately.²⁴⁻²⁶ In this manuscript, we consider one such limiting case for the compressible description of gases. We begin by deriving the equations of motion for a steady, irrotational, compressible flow in general orthogonal coordinates. This will be accomplished using two distinct formulations that rely either on the velocity potential or the streamfunction. We will also discuss the Rayleigh-Janzen asymptotic technique needed to solve these equations in the low-Mach number limit. While the procedure will be shown to be straightforward with the velocity potential, auxiliary relations will be required when using the streamfunction formulation. Finally, two particular case studies will be presented for the irrotational compressible flow in SRMs using both planar and axisymmetric settings.

II. Mathematical Formulation

To obtain the desired form of the compressible potential equation, proper normalization of variables must be effectuated. In what follows, starred variables allude to dimensional quantities, and subscripted parameters denote constants taken at reference conditions:

$$\begin{aligned} \mathbf{x} &= \frac{\mathbf{x}^*}{a_0}; & \mathbf{u} &= \frac{\mathbf{u}^*}{U_\infty}; & c &= \frac{c^*}{c_0}; & M_\infty &= \frac{U_\infty}{c_0} \\ \psi &= \frac{\psi^*}{U_\infty \rho_0 a_0}; & \phi &= \frac{\phi^*}{U_\infty a_0}; & \rho &= \frac{\rho^*}{\rho_0}; & p &= \frac{p^*}{p_0} \end{aligned} \tag{1}$$

To be specific, the reference values denote, successively: ρ_0 , the reference density, a_0 , some reference length (e.g. pipe radius or channel half height), U_∞ , the reference mean flow speed (e.g. sidewall injection or free stream speed), and c_0 , the reference speed of sound. For injection driven flows, the reference conditions may be taken at the injecting surfaces, whereas the free stream condition may be more convenient to designate as a benchmark for external flows.

A. Velocity Potential

In the interest of portability, vector notations will be maintained as much as possible. We start with the steady-state continuity equation for a compressible fluid of density ρ^* . This may be written as

$$\nabla^* \cdot (\rho^* \mathbf{u}^*) = 0 \quad (2)$$

Given that the flow is irrotational, the velocity field can be represented as the gradient of a scalar. Then, substituting $\mathbf{u}^* = \nabla^* \phi^*$ in Eq. (2), we can put

$$\nabla^* \cdot (\rho^* \nabla^* \phi^*) = 0 \quad (3)$$

or, more conveniently

$$\nabla^{*2} \phi^* = -\frac{1}{\rho^*} \nabla^* \phi^* \cdot \nabla^* \rho^* \quad (4)$$

It is clear from Eq. (3) that, when the flow is homogeneously incompressible (i.e. $\nabla^* \rho^* = \mathbf{0}$), the Laplace equation for incompressible irrotational flow is restored identically, viz. $\nabla^2 \phi = 0$.

The second step consists of expressing the gradient of the density in terms of the velocity potential ϕ^* . This may be arrived at by using the definition of the speed of sound. In dimensional form, we recall that

$$\frac{dp^*}{d\rho^*} \equiv c^{*2} \quad (5)$$

It follows that the density and pressure gradients remain intimately connected through

$$\nabla^* \rho^* = \frac{1}{c^{*2}} \nabla^* p^* \quad (6)$$

It may be important to remark that the speed of sound in Eq. (6) varies spatially, i.e. $c^* \equiv c^*(\mathbf{x})$. To complete the specification of the density in terms of the velocity potential, the Euler momentum equation may be approached to connect the pressure to the velocity. This is accomplished by setting

$$\nabla^* p^* = -\rho^* \mathbf{u}^* \cdot \nabla^* \mathbf{u}^* = -\rho^* \left(\frac{1}{2} \nabla^* \mathbf{u}^{*2} - \mathbf{u}^* \times \nabla^* \times \mathbf{u}^* \right) = -\frac{1}{2} \rho^* \nabla^* \mathbf{u}^{*2} \quad (7)$$

where the condition of irrotationality, $\nabla^* \times \mathbf{u}^* = \mathbf{0}$, has been used. By making proper substitutions into Eq. (3), we are left with

$$\nabla^{*2} \phi^* = \frac{1}{2c^{*2}} \nabla^* \phi^* \cdot \nabla^* \mathbf{u}^{*2} \quad (8)$$

This equation is identical to the compressible potential equation that appears in classic monographs on the subject.²⁷ To make further headway, the local speed of sound must be expressed in terms of the velocity potential and the free stream or reference condition. For this, we make use of the energy equation which, for irrotational motion, is characterized by a stagnation energy that stays invariant throughout the flowfield. Using h^* to denote the flow enthalpy, conservation of energy may be stated as

$$h^* + \frac{1}{2} \mathbf{u}^{*2} = h_0^* + \frac{1}{2} \mathbf{U}_0^{*2} = \text{const} \quad (9)$$

or

$$\frac{c^{*2}}{\gamma - 1} + \frac{1}{2} \mathbf{u}^{*2} = \frac{c_0^2}{\gamma - 1} + \frac{1}{2} \mathbf{U}_0^{*2} \quad (10)$$

A simple rearrangement of Eq. (10) yields

$$c^{*2} = c_0^2 + \frac{\gamma - 1}{2} \mathbf{U}_0^{*2} - \frac{\gamma - 1}{2} \mathbf{u}^{*2} \quad (11)$$

This relation enables us to connect the local speed of sound to the reference parameters and local velocity. It constitutes a crucial step in our analysis. By substituting c^* into Eq. (8), we get

$$c^{*2} \nabla^{*2} \phi^* = \left(c_0^2 + \frac{\gamma-1}{2} U_0^{*2} - \frac{\gamma-1}{2} \mathbf{u}^{*2} \right) \nabla^{*2} \phi^* = \frac{1}{2} \nabla^* \phi^* \cdot \nabla^* \mathbf{u}^{*2} \quad (12)$$

At this juncture, the normalization given in Eq. (1) may be inserted to obtain

$$\left(c_0^2 + \frac{\gamma-1}{2} U_\infty^2 U_0^2 - \frac{\gamma-1}{2} U_\infty^2 \mathbf{u}^2 \right) \frac{U_\infty}{a} \nabla^2 \phi = \frac{U_\infty^3}{2a} \nabla \phi \cdot \nabla \mathbf{u}^2 \quad (13)$$

Then, multiplying by a/U_∞^3 gives

$$\left(\frac{c_0^2}{U_\infty^2} + \frac{\gamma-1}{2} U_0^2 - \frac{\gamma-1}{2} \mathbf{u}^2 \right) \nabla^2 \phi = \nabla \phi \cdot \nabla \mathbf{u}^2 \quad (14)$$

Recognizing the inverted mean flow Mach number in the first member of Eq. (14), we multiply through by M_∞^2 and write

$$\left(1 + M_\infty^2 \frac{\gamma-1}{2} U_0^2 - M_\infty^2 \frac{\gamma-1}{2} \mathbf{u}^2 \right) \nabla^2 \phi = M_\infty^2 \nabla \phi \cdot \nabla \mathbf{u}^2 \quad (15)$$

We thus arrive at the following compact form,

$$\nabla^2 \phi = \frac{1}{2} M_\infty^2 \left[\nabla \phi \cdot \nabla \mathbf{u}^2 + (\gamma-1) (\mathbf{u}^2 \nabla^2 \phi - U_0^2 \nabla^2 \phi) \right] \quad (16)$$

In terms of the velocity potential, an equivalent expression is

$$\nabla^2 \phi = \frac{1}{2} M_\infty^2 \left\{ \nabla \phi \cdot \nabla [(\nabla \phi)^2] + (\gamma-1) (\nabla \phi)^2 \nabla^2 \phi - (\gamma-1) U_0^2 \nabla \phi \right\} \quad (17)$$

In most practical cases, the reference point is taken at the stagnation condition for which $\mathbf{U}_0 = \mathbf{0}$. Other possible reference values include conditions in the free stream or inlet plane where properties are fixed. In our case, Eq. (17) reduces to

$$\nabla^2 \phi = \frac{1}{2} M_\infty^2 \left\{ \nabla \phi \cdot \nabla [(\nabla \phi)^2] + (\gamma-1) (\nabla \phi)^2 \nabla^2 \phi \right\} \quad (18)$$

The Poisson equation given above provides the complete description of an irrotational compressible fluid in orthogonal coordinates. Its analytical solution warrants the use of limiting cases such as the low-Mach approximation. This is illustrated in Sec. III where the Rayleigh-Janzen expansion is detailed.

B. Streamfunction Formulation

For two-dimensional problems, the compressible equation of motion may be expressed in terms of the streamfunction. In this case, one may readily invoke the condition of irrotationality ($\boldsymbol{\Omega} \equiv \nabla \times \mathbf{u} = \mathbf{0}$) to extract an equation for the streamfunction. Having a single useful component perpendicular to the plane of motion, the vorticity for the planar flow problem may be written as

$$\Omega_z = \frac{\partial v}{\partial x} - \frac{\partial u}{\partial y} = 0 \quad (19)$$

where u and v denote the axial and transverse velocity components, respectively. One can introduce the compressible streamfunction using the standard definition,

$$u = \frac{1}{\rho} \frac{\partial \psi}{\partial y}; \quad v = -\frac{1}{\rho} \frac{\partial \psi}{\partial x} \quad (20)$$

Upon inserting Eq. (20) into Eq. (19), we obtain

$$\nabla^2 \psi = \frac{1}{\rho} \nabla \rho \cdot \nabla \psi \quad (21)$$

For axisymmetric motion in cylindrical coordinates, a similar analysis leads to

$$\nabla^2 \psi - \frac{2}{r} \frac{\partial \psi}{\partial r} = \frac{1}{\rho} \nabla \rho \cdot \nabla \psi \quad (22)$$

with

$$u = -\frac{1}{\rho r} \frac{\partial \psi}{\partial z}; \quad w = \frac{1}{\rho r} \frac{\partial \psi}{\partial r} \quad (23)$$

where u and w stand for the radial and axial velocities, respectively. Combining the planar and axisymmetric formulations into one, we get

$$D^2 \psi = \frac{1}{\rho} \nabla \rho \cdot \nabla \psi; \quad D^2 = \begin{cases} \frac{\partial^2}{\partial x^2} + \frac{\partial^2}{\partial y^2} & \text{planar} \\ \frac{\partial^2}{\partial r^2} - \frac{1}{r} \frac{\partial}{\partial r} + \frac{\partial^2}{\partial z^2} & \text{axisymmetric} \end{cases} \quad (24)$$

where D^2 is a differential operator whose form depends on the coordinate system under consideration. At this stage, the density gradient may be eliminated in favor of the streamfunction. By using Eq. (6), we extract

$$D^2 \psi = -\frac{M_\infty^2}{2c^2} \nabla \mathbf{u}^2 \cdot \nabla \psi \quad (25)$$

Finally, using Eq. (5), we obtain

$$D^2 \psi = \frac{1}{2}(\gamma - 1)M_\infty^2 \mathbf{u}^2 D^2 \psi - \frac{1}{2}M_\infty^2 \nabla \mathbf{u}^2 \cdot \nabla \psi \quad (26)$$

Equation (26) represents the streamfunction formulation for the steady, compressible, and irrotational two dimensional flow. Its solution may be sought by assuming a low Mach number in a regular perturbation expansion that will be illustrated next.

III. Low Mach Number Solution

The Rayleigh-Janzen expansion^{28,29} is a regular perturbation series in even (or odd) powers of the Mach number that is particularly suited for compressible flow problems. Majdalani¹⁵ and Maicke and Majdalani¹⁶ have successfully applied it to the compressible rotational flow in a porous cylinder and channel, respectively. In the case of the irrotational compressible field, a similar expansion is in order. In fact, one can justify the use of even powers of the Mach number by recognizing that, in Eqs. (18) and (24), the square of the Mach number appears explicitly. In this scheme, a scalar (or vector) φ may be decomposed as follows:

$$\varphi = \varphi_0 + M_\infty^2 \varphi_1 + M_\infty^4 \varphi_2 + \dots + M_\infty^{2N} \varphi_N + O(M_\infty^{2N+2}) = \sum_{n=0}^N M_\infty^{2n} \varphi_n + O(M_\infty^{2N+2}) \quad (27)$$

This expansion may be applied to the velocity potential as well as to the streamfunction.

A. Velocity Potential

In this situation, the velocity potential may be expressed as

$$\phi = \sum_{n=0}^N M_\infty^{2n} \phi_n + O(M_\infty^{2N+2}) \quad (28)$$

Its substitution into the velocity potential formulation given by Eq. (18) precipitates

$$O(0): \quad \nabla^2 \phi_0 = 0 \quad (29)$$

$$O(M_\infty^2): \quad \nabla^2 \phi_1 = \frac{1}{2} \nabla \phi_0 \cdot \nabla [(\nabla \phi_0)^2] \quad (30)$$

$$O(M_\infty^4): \quad \nabla^2 \phi_2 = \nabla \phi_0 \cdot \nabla (\nabla \phi_0 \cdot \nabla \phi_1) + \frac{1}{2} \nabla \phi_1 \cdot \nabla [(\nabla \phi_0)^2] \\ + \frac{1}{2}(\gamma - 1)(\nabla \phi_0)^2 \nabla^2 \phi_1 \quad (31)$$

⋮

Note that $\nabla^2\phi_0 = 0$ is employed to reduce the first and second orders in Eqs. (30) and (31). This set of equations is closed; with the specification of suitable boundary conditions, it offers a practical model for irrotational flow analysis. In the next section, we illustrate the procedure for obtaining an alternate perturbation solution using Eq. (24) as a starting point.

B. Streamfunction Formulation

In our quest for a perturbation approximation, it may be argued that Eq. (24) is more advantageous from an algebraic perspective. By applying the Rayleigh-Janzen expansion technique to all flowfield variables, an assortment of consecutive series is produced, namely,

$$\psi = \psi_0 + M_\infty^2\psi_1 + M_\infty^4\psi_2 + O(M_\infty^6) \quad (32)$$

$$\mathbf{u} = \mathbf{u}_0 + M_\infty^2\mathbf{u}_1 + M_\infty^4\mathbf{u}_2 + O(M_\infty^6) \quad (33)$$

$$p = 1 + M_\infty^2p_1 + M_\infty^4p_2 + O(M_\infty^6) \quad (34)$$

$$\rho = 1 + M_\infty^2\rho_1 + M_\infty^4\rho_2 + O(M_\infty^6) \quad (35)$$

The first three order of M_∞^2 yield ψ in powers of

$$O(0): \quad D^2\psi_0 = 0 \quad (36)$$

$$O(M_\infty^2): \quad D^2\psi_1 = \nabla\rho_1 \cdot \nabla\psi_0 \quad (37)$$

$$O(M_\infty^4): \quad D^2\psi_2 = -\rho_1\nabla^2\psi_1 + \nabla\rho_1 \cdot \nabla\psi_1 + \nabla\rho_2 \cdot \nabla\psi_0 \quad (38)$$

To close Eqs. (36)–(38), an approximation for the density is needed at every order. This can be achieved by invoking the isentropic relation

$$\rho = p^{1/\gamma} \quad (39)$$

Subsequently, by expanding the density and the pressure, we reape

$$O(0): \quad \rho_0 = 1 \quad (40)$$

$$O(M_\infty^2): \quad \rho_1 = \frac{p_1}{\gamma} \quad (41)$$

$$O(M_\infty^4): \quad \rho_2 = \frac{p_2}{\gamma} + \frac{1-\gamma}{2\gamma^2}p_1^2 \quad (42)$$

As for the pressure itself, a Rayleigh-Janzen expansion may be applied to the Euler momentum relation given by Eq. (7). This enables us to identify the first three orders for p , specifically

$$O(0): \quad \nabla p_0 = 0 \quad (43)$$

$$O(M_\infty^2): \quad \nabla p_1 = -\frac{1}{2}\gamma\rho_0\nabla\mathbf{u}_0^2 \quad (44)$$

$$O(M_\infty^4): \quad \nabla p_2 = -\frac{1}{2}\gamma\rho_1\nabla\mathbf{u}_0^2 - \gamma\nabla(\mathbf{u}_0 \cdot \mathbf{u}_1) \quad (45)$$

Clearly, the solution using the streamfunction requires evaluation of the pressure, density, and velocity at every consecutive order. This additional effort appears to be more labor-intensive than using the velocity potential formulation in which these properties are simply bypassed. Nonetheless, it must be borne in mind that the pressure and density remain of primary interest and so their evaluation will be required at some point even when using the velocity potential.

IV. Case Studies

In order to illustrate the usefulness of the orthogonal coordinate formulation, two case studies are considered and tracked from initial treatment to final expression. Both studies employ symmetry assumptions to reduce the domain to a two-dimensional form so that both the potential and streamfunction approaches may be employed. For three-dimensional problems, only the potential formulation will be viable.

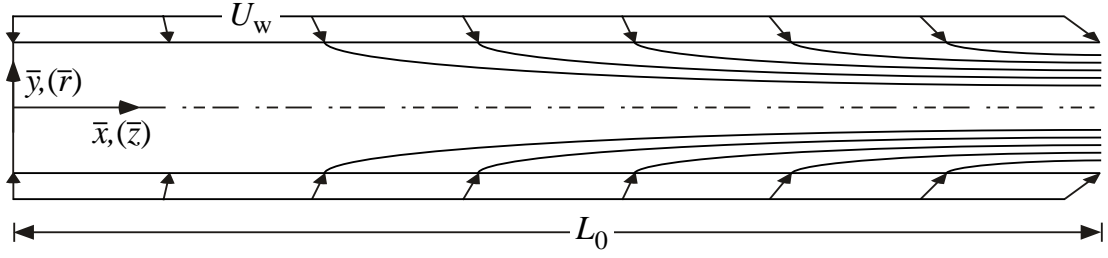


Figure 1. Schematic of the planar and axisymmetric motor configurations where cylindrical coordinates are listed between parentheses.

A. Planar Case of a Slab Rocket Motor

The slab or rectangular rocket motor, though rarely considered for commercial applications, remains of direct relevance to theoretical^{30,31} and experimental researchers.^{32,33} A schematic of the system is provided in Fig. 1. The geometric setting gives rise to a simplified set-up for data acquisition, visualization, and modeling, while still retaining many of the essential features of the problem under investigation. The corresponding analytical model is comprised of a rectangular channel of half-height a_0 and length L_0 . The top and bottom walls allow injection at a constant velocity U_w while the headwall remains impermeable. Symmetry justifies a domain reduction to a half-chamber when the coordinate system is placed judiciously at the center of the headwall. By taking the half-height as the characteristic length according to Eq. (1), the domain is rescaled to $0 \leq x \leq L$ and $0 \leq y \leq 1$, where $L = L_0/a_0$. As for the boundary conditions, they are given by:

$$v(x, 0) = \frac{\partial \phi(x, 0)}{\partial y} = 0 \quad (\text{symmetry condition}); \quad \phi(0, 0) = 0 \quad (\text{potential datum}) \quad (46)$$

$$v(x, 1) = \frac{\partial \phi(x, 1)}{\partial y} = -1 \quad (\text{sidewall injection}); \quad u(0, y) = \frac{\partial \phi(0, y)}{\partial x} = 0 \quad (\text{inert headwall}) \quad (47)$$

These equalities must be imposed at the leading order only. For subsequent corrections, a zero right-hand-side is used lest the base solution is unduly modified.

1. Potential Solution

The analysis begins by expressing Eq. (29) in rectangular coordinates, namely,

$$\frac{\partial^2 \phi_0}{\partial x^2} + \frac{\partial^2 \phi_0}{\partial y^2} = 0 \quad (48)$$

This, after separation of variables, produces the familiar polynomial,

$$\phi_0 = \frac{1}{2} \nu x^2 + C_1 x + C_2 - \frac{1}{2} \nu y^2 + C_3 y + C_4 \quad (49)$$

Here ν is the leading-order separation constant. By virtue of Eq. (46), we find $C_3 = 0$. Subsequently, the potential datum eliminates the constants C_2 and C_4 . Then, the separation constant becomes $\nu = 1$ due to Eq. (47) and, lastly, the inert headwall boundary condition renders $C_1 = 0$. The resulting leading-order potential solution becomes

$$\phi_0 = \frac{1}{2} (x^2 - y^2) \quad (50)$$

With the leading-order potential fully determined, the pressure correction may be obtained directly from the first-order momentum equation, specifically from Eq. (44) in Cartesian coordinates:

$$\nabla p_1 = -\frac{1}{2} \gamma \nabla \left[\left(\frac{\partial \phi_0}{\partial x} \right)^2 + \left(\frac{\partial \phi_0}{\partial y} \right)^2 \right] \quad (51)$$

After integration, the pressure correction becomes

$$p_1 = -\frac{1}{2}\gamma(x^2 + y^2) \quad (52)$$

Having determined ϕ_0 and its derivatives, the first compressible correction to the potential function may be retrieved from Eq. (30). After converting the vector form into rectangular coordinates, we find

$$\frac{\partial^2 \phi_1}{\partial x^2} + \frac{\partial^2 \phi_1}{\partial y^2} = \frac{1}{2} \left(\frac{\partial \phi_0}{\partial x} \hat{x} + \frac{\partial \phi_0}{\partial y} \hat{y} \right) \cdot \left[\left(2 \frac{\partial \phi_0}{\partial x} \frac{\partial^2 \phi_0}{\partial x^2} + 2 \frac{\partial \phi_0}{\partial y} \frac{\partial^2 \phi_0}{\partial x \partial y} \right) \hat{x} + \left(2 \frac{\partial \phi_0}{\partial x} \frac{\partial^2 \phi_0}{\partial x \partial y} + 2 \frac{\partial \phi_0}{\partial y} \frac{\partial^2 \phi_0}{\partial y^2} \right) \hat{y} \right] \quad (53)$$

where the right-hand-side members collapse into

$$\frac{\partial^2 \phi_1}{\partial x^2} + \frac{\partial^2 \phi_1}{\partial y^2} = \left(\frac{\partial \phi_0}{\partial x} \right)^2 \frac{\partial^2 \phi_0}{\partial x^2} + 2 \frac{\partial \phi_0}{\partial x} \frac{\partial \phi_0}{\partial y} \frac{\partial^2 \phi_0}{\partial x \partial y} + \left(\frac{\partial \phi_0}{\partial y} \right)^2 \frac{\partial^2 \phi_0}{\partial y^2} \quad (54)$$

Since the leading-order potential function contains no mixed products of x and y , the mixed derivatives vanish; we are left with

$$\frac{\partial^2 \phi_1}{\partial x^2} + \frac{\partial^2 \phi_1}{\partial y^2} = x^2 - y^2 \quad (55)$$

Using an additive rather than multiplicative separation of variables ansatz, we extract

$$\phi_1 = \frac{1}{12}x^4 + \frac{1}{2}\kappa x^2 + K_1 x + K_2 - \frac{1}{12}y^4 - \frac{1}{2}\kappa y^2 + K_3 x + K_4 \quad (56)$$

The boundary conditions may be applied in the same manner as the leading order, though in this instance a null value is enforced on the right-hand-side of all conditions to ensure that the solution at any order fulfills the same physical requirements. This process results in all of the K constants vanishing except for the separation constant, $\kappa = -\frac{1}{3}$. The complete first-order potential function becomes

$$\phi_1 = \frac{1}{12}(x^4 - y^4) + \frac{1}{6}(y^2 - x^2) \quad (57)$$

The pressure companion may be readily determined from Eq. (45) through substitution and integration of the (ϕ_0, ϕ_1) pair; the second-order pressure is found to be

$$p_2 = \gamma \left[\frac{1}{4}x^2 y^2 + \frac{1}{3}(x^2 + y^2) - \frac{5}{24}(x^4 + y^4) \right] \quad (58)$$

2. Streamfunction Solution

The procedure for determining the streamfunction is analogous to that used for the potential function. The geometric set-up is identical, as are the boundary conditions, though they must be adapted to the streamfunction formulation. Following the definition of ψ given by Eq. (23), we have

$$v_0(x, 0) = \frac{\partial \psi_0(x, 0)}{\partial x} = 0; \quad \psi_0(0, 0) = 0 \quad (59)$$

$$v_0(x, 1) = \frac{\partial \psi_0(x, 1)}{\partial x} = 1; \quad u_0(0, y) = \frac{\partial \psi(x, 0)}{\partial y} = 0 \quad (60)$$

The ψ_0 -equation, when expressed in rectangular coordinates, emerges as an expression of a vanishing Laplacian,

$$\frac{\partial^2 \psi_0}{\partial x^2} + \frac{\partial^2 \psi_0}{\partial y^2} = 0 \quad (61)$$

While this form is identical to that of the potential equation at leading order, it may be inferred by the change in boundary conditions that a different solution will be achieved here. Using multiplicative separation of variables and applying Eqs. (59)–(60), we promptly deduce

$$\psi_0 = xy \quad (62)$$

Before addressing the first-order correction, the pressure and the density must be specified. Because the same fundamental assumptions are used for the potential and streamfunction cases, one can simply use the pressure according to Eq. (52). Alternatively, the pressure may be found by substituting the streamfunction definitions for the velocity terms into Eq. (44). Both methods return the same result. Once the pressure is known, the density may be deduced from the isentropic relation. In this case, Eq. (42) yields

$$\rho_1 = -\frac{1}{2}(x^2 + y^2) \quad (63)$$

With ρ_1 in hand, the first compressible correction to ψ may be pursued. Expressed in the Cartesian coordinate system, we have

$$\frac{\partial^2 \psi_1}{\partial x^2} + \frac{\partial^2 \psi_1}{\partial y^2} = \frac{\partial \rho_1}{\partial x} \frac{\partial \psi_0}{\partial x} + \frac{\partial \rho_1}{\partial y} \frac{\partial \psi_0}{\partial y} \quad (64)$$

The auxiliary conditions on the first-order correction are more elaborate as they involve both the density and the streamfunction. They beget:

$$v_1(x, 0) = \frac{\partial \psi_1(x, 0)}{\partial x} - \rho_1 \frac{\partial \psi_0(x, 0)}{\partial x} = 0; \quad \psi_1(0, 0) = 0 \quad (65)$$

$$v_1(x, 1) = \frac{\partial \psi_1(x, 1)}{\partial x} - \rho_1 \frac{\partial \psi_0(x, 1)}{\partial x} = 0; \quad u_1(0, y) = \frac{\partial \psi_1(0, y)}{\partial y} - \rho_1 \frac{\partial \psi_0(0, y)}{\partial y} = 0 \quad (66)$$

At this point in the analysis, the terms on the right-hand-side of Eqs. (64)–(66) are already known. Their backward substitution leads to

$$\frac{\partial^2 \psi_1}{\partial x^2} + \frac{\partial^2 \psi_1}{\partial y^2} = -2xy \quad (67)$$

which is subject to

$$v_1(x, 0) = \frac{\partial \psi_1(x, 0)}{\partial x} = 0; \quad \psi_1(0, 0) = 0 \quad (68)$$

$$u_1(0, y) = \frac{\partial \psi_1(0, y)}{\partial y} = 0; \quad v_1(x, 1) = \frac{\partial \psi_1(x, 1)}{\partial x} = -\frac{1}{2} - \frac{x^2}{2} \quad (69)$$

With the boundary conditions serving as a guide, the solution may be inferred to be a combination of the homogenous and particular parts, namely,

$$\psi_1 = a_0 + a_1 xy + a_2 x^3 y + a_3 xy^3 \quad (70)$$

At length, judicious application of the boundary conditions reveals

$$\psi_1 = -\frac{1}{3}xy - \frac{1}{6}(x^3 y + xy^3) \quad (71)$$

B. Axisymmetric Case of a Cylindrical Rocket Motor

The potential flow in a cylindrical rocket motor was first addressed by the authors³⁴ without the benefit of the generalized framework. It is presented here as an additional avenue for validating the coordinate-independent formulation. The geometry consists of a right rectangular cylinder of radius a_0 and length L_0 . The sidewalls of the cylinder are permeable, permitting a constant radial injection, U_w . The origin is placed at the center of the inert headwall and symmetry enables us to reduce the domain to the region delineated by $0 \leq r \leq 1$ and $0 \leq z \leq L$, where the reference length employed is the radius of the chamber. Mathematically these boundary conditions translate into

$$u_r(0, z) = \frac{\partial \phi(0, z)}{\partial r} = 0; \quad \phi(0, 0) = 0 \quad (72)$$

$$u_z(r, 0) = \frac{\partial \phi(r, 0)}{\partial z} = 0; \quad u_r(1, z) = \frac{\partial \phi(1, z)}{\partial r} = -1 \quad (73)$$

In keeping with perturbation theory, these conditions are enforced at the leading order only; as usual, null conditions are applied at subsequent orders everywhere else.

1. Potential Solution

To initiate the solution for the circular-port chamber, Eq. (29) may be expanded in cylindrical coordinates viz.

$$\frac{\partial^2 \phi_0}{\partial r^2} + \frac{1}{r} \frac{\partial \phi_0}{\partial r} + \frac{\partial^2 \phi_0}{\partial z^2} = 0 \quad (74)$$

The outcome may be inferred using additive separation of variables; we get

$$\phi_0 = \frac{1}{4} \nu r^2 + C_1 \ln r + C_2 - \frac{1}{2} \nu z^2 + C_3 z + C_4 \quad (75)$$

As with the slab rocket motor case, the boundary conditions result in all constants vanishing except for the $\nu = -2$ value that may be retrieved from Eq. (73). The axisymmetric leading-order potential becomes

$$\phi_0 = -\frac{1}{2} r^2 + z^2 \quad (76)$$

Next, the thermodynamic variables p_1 and ρ_1 may be extracted from the momentum and the isentropic relations, respectively. Beginning with Eq. (44) and expanding in scalar form, we find

$$\nabla p_1 = -\frac{1}{2} \gamma \nabla \left[\left(\frac{\partial \phi_0}{\partial r} \right)^2 + \left(\frac{\partial \phi_0}{\partial z} \right)^2 \right] \quad (77)$$

whose integration yields

$$p_1 = -\frac{1}{2} \gamma (r^2 + 4z^2) \quad (78)$$

It may hence be seen that compressibility effects are first introduced in the first-order correction. The coordinate-independent equation at the first order, when written in terms of (r, z) , unfolds into

$$\frac{\partial^2 \phi_1}{\partial r^2} + \frac{1}{r} \frac{\partial \phi_1}{\partial r} + \frac{\partial^2 \phi_1}{\partial z^2} = \left(\frac{\partial \phi_0}{\partial r} \right)^2 \frac{\partial^2 \phi_0}{\partial r^2} + 2 \frac{\partial \phi_0}{\partial r} \frac{\partial \phi_0}{\partial z} \frac{\partial^2 \phi_0}{\partial r \partial z} + \left(\frac{\partial \phi_0}{\partial z} \right)^2 \frac{\partial^2 \phi_0}{\partial z^2} \quad (79)$$

For this particular case, no terms in ϕ_0 contain products of r and z , so the mixed derivatives vanish identically. Inserting Eq. (76) at the right-hand-side of Eq. (79) leaves us with

$$\frac{\partial^2 \phi_1}{\partial r^2} + \frac{1}{r} \frac{\partial \phi_1}{\partial r} + \frac{\partial^2 \phi_1}{\partial z^2} = -r^2 + 8z^2 \quad (80)$$

Once again, an additive separation of variables may be employed to deliver

$$\phi_1 = \kappa \frac{r^2}{4} - \frac{r^4}{16} + K_1 \ln r + K_2 + \frac{2}{3} z^4 - \frac{\kappa}{2} z^2 + K_3 z + K_4 \quad (81)$$

Here κ is the first-order separation constant. As before, the null auxiliary conditions may be imposed to the extent of retrieving

$$\phi_1 = \frac{r^2}{8} - \frac{r^4}{16} + \frac{2}{3} z^4 - \frac{z^2}{4} \quad (82)$$

Consequently, the compressible pressure correction may be produced from Eq. (45) where direct integration renders

$$p_2 = -\gamma \left[\frac{1}{8} (r^4 - 2r^2) - r^2 z^2 + \frac{10}{3} z^4 - z^2 \right] \quad (83)$$

2. Streamfunction Solution

Given no variations in the azimuthal direction, the streamfunction approach may be resorted to as a viable alternative in cylindrical coordinates. The leading-order equation in this case changes to

$$\frac{\partial^2 \psi_0}{\partial r^2} - \frac{1}{r} \frac{\partial \psi_0}{\partial r} + \frac{\partial^2 \psi_0}{\partial z^2} = 0 \quad (84)$$

It may be important to note the sign switch in the second member of Eq. (84); the minus sign distinguishes this expression from its potential counterpart. This particular change in sign is what justifies the use of D^2 in lieu of ∇^2 in the streamfunction formulation. After separation of variables and application of the requisite conditions, the leading-order streamfunction emerges, namely,

$$\psi_0 = r^2 z \quad (85)$$

Afterwards, the pressure term may be derived from the potential solution or solved independently using the momentum equation written in terms of ψ . Both methods lead to Eq. (78). The density can then be evaluated from the isentropic relation,

$$\rho_1 = -\frac{1}{2}(r^2 + 4z^2) \quad (86)$$

With the density term in hand, the first-order streamfunction equation reduces to

$$\frac{\partial^2 \psi_1}{\partial r^2} - \frac{1}{r} \frac{\partial \psi_1}{\partial r} + \frac{\partial^2 \psi_1}{\partial z^2} = -6r^2 z \quad (87)$$

Its solution, after separation of variables and application of homogeneous conditions, collapses into

$$\psi_1 = -\frac{1}{4}r^2 z - \frac{1}{4}r^4 z - \frac{2}{3}r^2 z^3 \quad (88)$$

V. Results and Discussion

Before proceeding with the results, a summary of the key relations is provided to enhance clarity. For planar flow in a slab motor, the principle variables may be evaluated from

$$\phi = \frac{1}{2}(x^2 - y^2) + \left[\frac{1}{12}(x^4 - y^4) + \frac{1}{6}(y^2 - x^2) \right] M_\infty^2 \quad (89)$$

$$\psi = xy + \left[-\frac{1}{3}xy - \frac{1}{6}(x^2 + y^2)xy \right] M_\infty^2 \quad (90)$$

$$p = 1 - \frac{\gamma}{2}(x^2 + y^2) M_\infty^2 + \gamma \left[\frac{1}{4}x^2 y^2 + \frac{1}{3}(x^2 + y^2) - \frac{5}{24}(x^4 + y^4) \right] M_\infty^4 \quad (91)$$

$$\rho = 1 - \frac{1}{2}(x^2 + y^2) M_\infty^2 \quad (92)$$

$$u = x + \frac{1}{3}(x^2 - 1)xM_\infty^2; \quad v = -y + \frac{1}{3}(1 - y^2)yM_\infty^2 \quad (93)$$

Similarly, for the cylindrical case we find

$$\phi = -\frac{1}{2}r^2 + z^2 + \left[\frac{1}{16}(2 - r^2)r^2 + \frac{1}{12}(8z^2 - 3)z^2 \right] M_\infty^2 \quad (94)$$

$$\psi = r^2 z - \frac{1}{12} \left[3(1 - r^2) - 8z^2 \right] r^2 z M_\infty^2 \quad (95)$$

$$p = 1 - \frac{\gamma}{2}(r^2 + 4z^2) M_\infty^2 - \gamma \left[\frac{1}{8}(r^4 - 2r^2) - r^2 z^2 + \frac{10}{3}z^4 - z^2 \right] M_\infty^4 \quad (96)$$

$$\rho = 1 - \frac{1}{2}(r^2 + 4z^2) M_\infty^2 \quad (97)$$

$$u = -r + \frac{1}{4}(1 - r^2)rM_\infty^2; \quad w = 2z + \frac{1}{6}(16z^2 - 3)zM_\infty^2 \quad (98)$$

A. Velocity Profiles

Velocity profiles are often a focus in the investigation of new flowfield models; presently, the axial and normal velocity profiles are showcased in Fig. 2. For both geometric configurations, the velocities are uniquely determined from a single spatial coordinate that varies in the direction of the velocity itself. The graph also features the

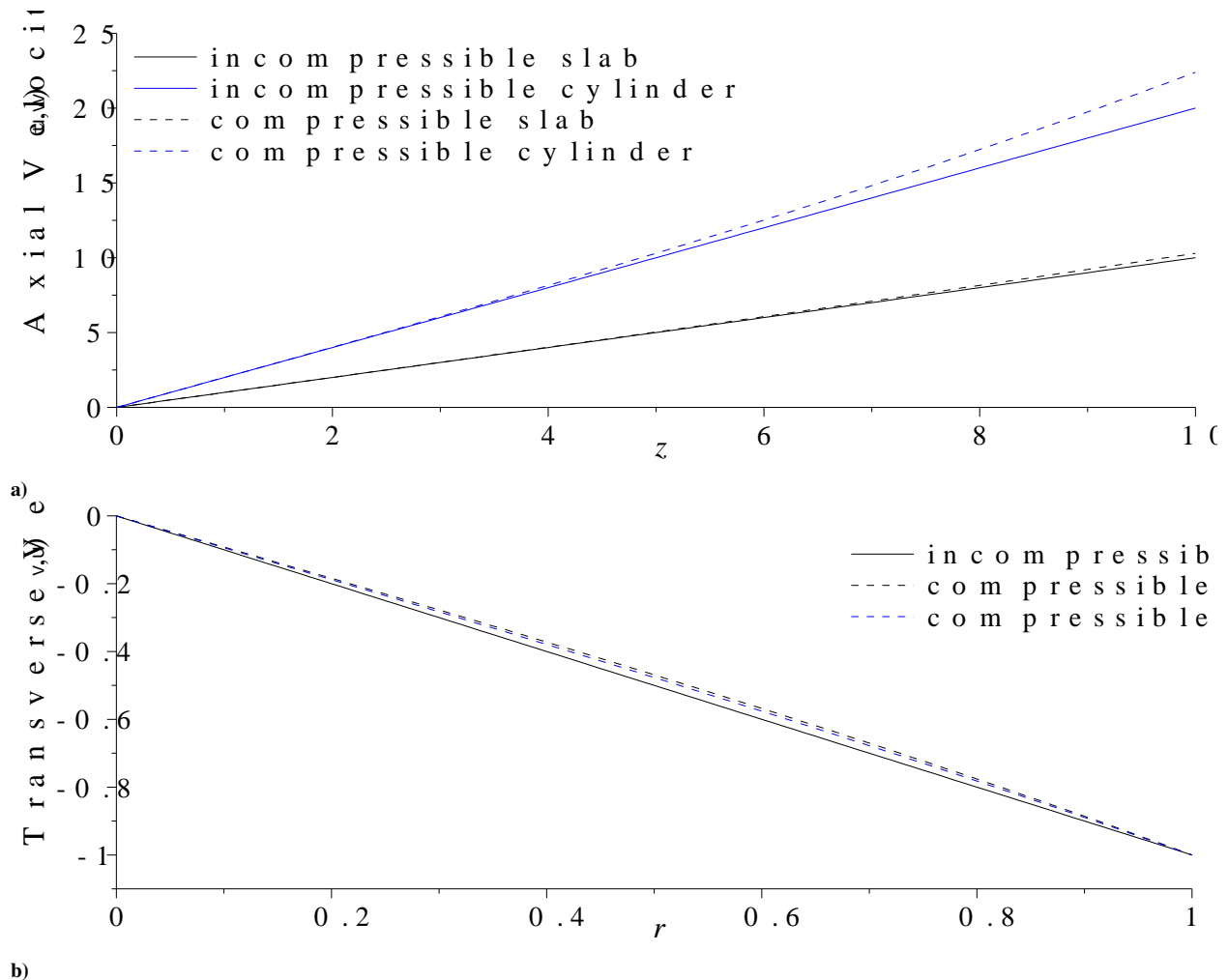


Figure 2. Axial and transverse velocity profiles for the slab and cylindrical rocket motors.

incompressible potential solution that behaves linearly. In comparison, the compressible corrections are seen to exhibit a polynomial form that introduces a slight curvature to the baseline profile. When compared to the incompressible case, the axial velocity experiences a small reduction at the headwall of the chamber before growing larger as the flow develops down the length of the chamber. As for the transverse speed, it matches the baseline approximation (and hence, the boundary conditions) at both ends of the domain, although its absolute value slightly diminishes for $0 < r < 1$. The compressible contribution is largest in the middle of the domain, specifically at $r = y = 1/\sqrt{3} \approx 0.57735$.

In comparing the planar and cylindrical results, some notable differences may be reported. First, the incompressible velocity in the axial direction is twice as large for the cylindrical chamber as it is for the slab. This result is consistent with the findings of Maicke and Majdalani.¹⁶ The doubling in speed may be ascribed to the additional mass injection that augments the flow in the cylindrical case. In contrast to the porous cylinder which is surrounded by injecting surfaces, the slab motor only permits injection from its top and bottom walls. This phenomenon is also exhibited in the compressible correction, as the first-order cylindrical term is approximately eight times as large as its Cartesian counterpart. While the normal velocities for the cylinder and slab are identical, their compressible contributions differ. In this instance, the slab normal velocity is one-third as large as the radial speed in the cylindrical chamber; nonetheless, the contribution of compressibility to the transverse velocity appears to be too small to be discerned graphically, or to pose a practical concern.

B. Critical Length

In former analyses of the sort developed here, a helpful practice has been to look for quantities that can offer deeper insight into the physics of the problem or provide new avenues for comparison. In the context of rocket motors, one such quantity is the critical length. The critical length, L_s , refers to the distance from the headwall to where the axial velocity first reaches sonic conditions. It also provides a functional limit to the present domain especially that the foregoing analysis precludes supersonic behavior. Estimating the critical length can be achieved through the dimensionless equation,

$$u^2 M_\infty^2 = T \quad (\text{planar}) \quad \text{or} \quad w^2 M_\infty^2 = T \quad (\text{axisymmetric}) \quad (99)$$

where the equations are written for Cartesian and cylindrical coordinates, respectively. The analyses for both relations are nearly identical, so the planar flow treatment will be illustrated first, followed by a summary of both cases. To begin, Eq. (99) is expanded in both velocity and temperature while retaining a balance in the truncation error. We get

$$u_0^2 M_\infty^2 + u_0 u_1 M_\infty^4 + u_1^2 M_\infty^6 = 1 + T_1 M_\infty^2 + T_2 M_\infty^4 \quad (100)$$

Next, we substitute the appropriate approximations for the velocity and temperature and ignore secondary variations in the radial direction. We obtain

$$x^2 M_\infty^2 + \frac{1}{3} (x^2 - 1) x^2 M_\infty^4 + \left[\frac{1}{3} (x^2 - 1) x \right]^2 M_\infty^6 = 1 - \frac{\gamma - 1}{2} x^2 M_\infty^2 + T_2 M_\infty^4 \quad (101)$$

This equation is a cubic polynomial in x^2 that can be solved explicitly. Recognizing that the full form is rather cumbersome, an asymptotic equivalent is pursued in lieu of an exact expression. Within the margin of error associated with the start-up relation, we find, for the planar geometry,

$$L_s = \sqrt{\frac{2}{3} - \frac{\gamma + 1}{M_\infty^2} + \frac{3(2\gamma^2 + \gamma - 1) - 2(\gamma + 1)M_\infty^2 + 2M_\infty^4 + 3\alpha^2/\sqrt[3]{2}}{3\sqrt[3]{2}\alpha M_\infty^2}} \quad (102)$$

For the cylindrical case, the equivalent expression reads

$$L_s = \sqrt{\frac{1}{8} - \frac{\gamma + 1}{4M_\infty^2} + \frac{8(2\gamma^2 + \gamma - 1) - 4(\gamma + 1)M_\infty^2 + M_\infty^4 + 4\sqrt[3]{4}\alpha^2}{32\sqrt[3]{2}\alpha M_\infty^2}} \quad (103)$$

Here α appears as a constant that is uniquely determined by the specific heat ratio; interestingly, the same α is unraveled in both planar and axisymmetric configurations. It is found to be

$$\alpha = [23 + 6\gamma - 3\gamma^2 - 4\gamma^3 + 3\sqrt{59 + 30\gamma - 12\gamma^2 - 22\gamma^3 - 3\gamma^4}]^{1/3} \quad (104)$$

The two expressions for L_s are compared in Fig. 3. As one may infer from the source equations, L_s will exhibit a weak sensitivity to the ratio of specific heats; however, this dependence will only slightly shifts the curves up or down with successive excursions in γ . At the outset, only a single case, $\gamma = 1.4$, is shown here. By analogy to the Hagen-Poiseuille flows in rectangular channels and circular tubes, the flowfield in the planar motor takes approximately twice as long as the axisymmetric flow to cross the critical length.^{35,36} This is also consistent with the findings of the previous section where the motion in a porous cylindrical was shown to exhibit twice the speed achieved at the same axial location in a porous channel.

C. Pressure

With the critical length in hand, it is possible to not only compare the planar and axisymmetric models to each other, but also to existing studies. To this end, comparison of the present work to a number of other axisymmetric studies is furnished in Fig. 4. The Taylor-Culick^{22,37} solution refers to the incompressible, rotational motion in widespread use, while the Majdalani study¹⁵ alludes to the compressible extension achieved using the Rayleigh-Janzen perturbation method. We also feature the model employed by Gany and Aharon,³⁸ albeit a one-dimensional representation that defines the pressure solely in terms of the axial coordinate and γ . Two numerical simulations also listed are borrowed from Majdalani¹⁵ and have been acquired using a finite volume Navier-Stokes solver.

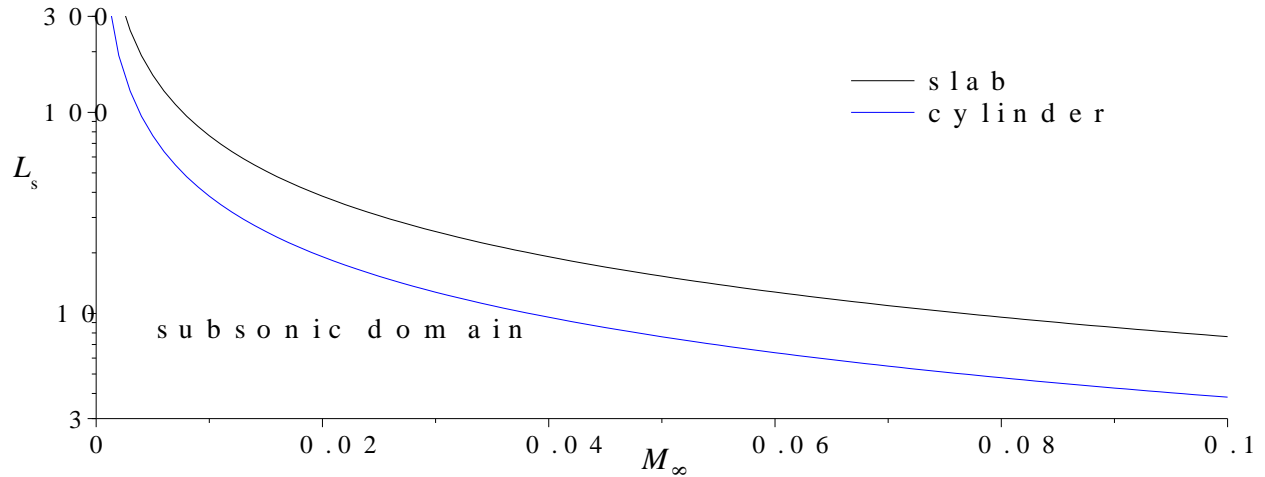


Figure 3. Critical length comparison between the slab and cylindrical cases.

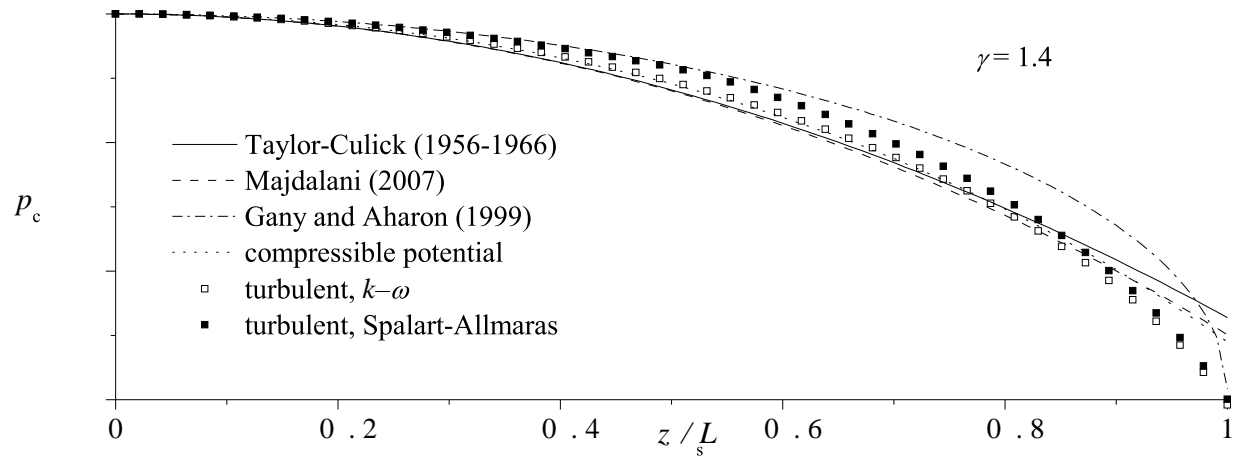


Figure 4. Centerline pressure compared to with existing studies of the axisymmetric flow configuration.

It may be gratifying to note that when normalized by the critical distance, the Cartesian and cylindrical potential pressures become virtually identical; graphically, they collapse onto the same curve. This behavior is not entirely surprising as the solutions are fundamentally similar in nature, differing only by constant multipliers. Employing the critical length in the axial normalization serves as a catalyst that effectively cancels these differences in the two solutions. When compared to the other analytical models, the pressure distribution shows excellent agreement both in shape of the pressure curves and in the actual values displayed. The only real outlier belongs to the one-dimensional approximation of Gany and Aharon³⁸ where a slightly different profile is seen. This can be attributed to the lack of two-dimensional effects in their velocity and pressure formulations.

VI. Conclusions

In this work, the potential equations of motion are reconstructed using a universal form that makes them applicable to two and three-dimensional flowfields, both internal and external, in a coordinate-independent framework. Two distinct formulations are advanced, one based on the potential velocity representation, and the other utilizing the streamfunction definition. While the former is applicable to multidimensional configurations, the latter is limited to two-dimensional flows that exhibit some type of symmetry or redundancy in one spatial direction. Both formulations

are presented using a form that is amenable to direct asymptotic treatment.

By way of example, two specific test cases are considered, and these have been traditionally associated with the irrotational inviscid motion in rocket chambers.^{39,40} Then using a regular Rayleigh-Janzen perturbation expansion in the Mach number squared, asymptotic approximations that are accurate to the fourth order in M_∞ are constructed independently for the planar and axisymmetric chamber geometries. Furthermore, these approximations are arrived at using both potential and streamfunction representations, thus helping to establish their equivalence in providing identical solutions to compressible flow problems.

Despite their relative simplicity, the two case studies considered here appear to be in good agreement with both lower and higher order models found in the literature. The assumption of irrotationality results in limited agreement over the shape of velocity profiles, but the ease of solution determination from the compressible potential equations makes this formulation ideal in some contexts, such as those concerned with a particular type of stability analysis. It should also be mentioned that the Rayleigh-Janzen technique employed here is only one possible solution method. Other analytical or numerical techniques,⁴¹ such as integral analysis and the Abel transform used by Akiki and Majdalani,^{17,18} could be used to obtain solutions that do not require the low Mach number constraint.

One of the most significant achievements here stands, perhaps, in the manner through which the compressible potential equations are recast into a formulation wherein the local speed of sound is eliminated in favor of its stagnation value. This enables us to introduce the constant mean flow Mach number at the basis of a perturbation expansion. It is hoped that the present framework will open up new avenues for research particularly in the investigation of yet undetermined compressible potentials, in two and three-dimensional space. More advanced engine concepts, such as those incorporating swirling motion, may now be treated with the newly developed methods. Finally, despite our emphasis on modeling internally burning motors in planar and cylindrical settings, the potential and streamfunction formulations outlined here can be just as easily applied to obtain compressible corrections to a large variety of internal and external flows, such as those cataloged in the NACA airfoil library. It is hoped that their treatment will receive attention in future work.

Acknowledgments

This material is based on work supported partly by the National Science Foundation through Grant No. CMMI-0928762, and partly by the University of Tennessee Space Institute, through institutional cost sharing.

References

- ¹Anderson, J. D., *Modern Compressible Flow with Historical Perspective*, McGraw-Hill, New York, NY, New York, 3rd ed., 2003.
- ²Barber, T. A., Maicke, B. A., and Majdalani, J., "Current State of High Speed Propulsion: Gaps, Obstacles, and Technological Challenges in Hypersonic Applications," *45th AIAA/ASME/SAE/ASEE Joint Propulsion Conference and Exhibit*, AIAA Paper 2009-5118, Denver, Colorado, August 2009.
- ³Cruise, D. R., "Notes on the Rapid Computation of Chemical Equilibria," *The Journal of Physical Chemistry*, Vol. 68, No. 12, 1964, pp. 3797–3802. doi:10.1021/j100794a044.
- ⁴Billig, F., "Design of Supersonic Combustors Based on Pressure-Area Fields," *Symposium (International) on Combustion*, Vol. 11, No. 1, 1967, pp. 755–769. doi:10.1016/S0082-0784(67)80201-7.
- ⁵Maicke, B. A., Barber, T. A., and Majdalani, J., "Evaluation of CFD Codes for Hypersonic Flow Modeling," *46th AIAA/ASME/SAE/ASEE Joint Propulsion Conference and Exhibit*, AIAA Paper 2010-7184, Nashville, Tennessee, July 2010.
- ⁶Maicke, B. A., Barber, T. A., and Majdalani, J., "Analytical Methodologies for Hypersonic Propulsion," *46th AIAA/ASME/SAE/ASEE Joint Propulsion Conference and Exhibit*, AIAA Paper 2010-6553, Nashville, Tennessee, July 2010.
- ⁷Liepmann, H. W., and Roshko, A., *Elements of Gasdynamics*, Dover Publications, New York, NY, 2001.
- ⁸Nigro, N., Storti, M., and Idelsohn, S., "GMRES Physics-Based Preconditioner For All Reynolds and Mach Numbers: Numerical Examples," *International Journal for Numerical Methods in Fluids*, Vol. 25, No. 12, December 1997, pp. 1347–1371. doi:10.1002/(SICI)1097-0363(19971230)25:12<1347::AID-FLD608>3.0.CO;2-C.
- ⁹Rauwoens, P., Vierendeels, J., Dick, E., and Merci, B., "A Conservative Pressure-Correction Scheme for Transient Simulations of Reacting Flows," *Journal of Computational and Applied Mathematics*, Vol. 234, No. 7, August 2010, pp. 2311–2318. doi:10.1016/j.cam.2009.08.087.
- ¹⁰Mary, I., Sagaut, P., and Deville, M., "An Algorithm for Low Mach Number Unsteady Flows," *Computers and Fluids*, Vol. 29, No. 2, February 2000, pp. 119–147. doi:10.1016/S0045-7930(99)00007-9.
- ¹¹Sand, I., "On Unsteady Reacting Flow in a Channel with a Cavity," *Journal of Fluid Mechanics*, Vol. 229, August 1991, pp. 339–364. doi:10.1017/S0022112091003051.
- ¹²Nicoud, F., "Conservative High-Order Finite-Difference Schemes for Low-Mach Number Flows," *Journal of Computational Physics*, Vol. 158, No. 1, February 2000, pp. 71–97. doi:10.1006/jcph.1999.6408.
- ¹³Rauwoens, P., Vierendeels, J., and Merci, B., "A Stable Pressure-Correction Scheme for Variable Density Flows Involving Non-Premixed Combustion," *International Journal for Numerical Methods in Fluids*, Vol. 56, No. 8, March 2008, pp. 1465–1471. doi:10.1002/flid.1717.

- ¹⁴Dokumaci, E., “On Transmission of Sound in a Non-Uniform Duct Carrying a Subsonic Compressible Flow,” *Journal of Sound and Vibration*, Vol. 210, No. 3, February 1998, pp. 391–401. doi:10.1006/jsvi.1997.1335.
- ¹⁵Majdalani, J., “On Steady Rotational High Speed Flows: The Compressible Taylor–Culick Profile,” *Proceedings of the Royal Society A: Mathematical, Physical and Engineering Science*, Vol. 463, No. 2077, January 2007, pp. 131–162. doi:10.1098/rspa.2006.1755.
- ¹⁶Maicke, B. A., and Majdalani, J., “On the Rotational Compressible Taylor Flow in Injection-Driven Porous Chambers,” *Journal of Fluid Mechanics*, Vol. 603, No. 1, May 2008, pp. 391–411. doi:10.1017/S002211200800112.
- ¹⁷Akiki, M., and Majdalani, J., “Compressibility Effects in Slender Rocket Motors,” *45th AIAA/ASME/SAE/ASEE Joint Propulsion Conference and Exhibit*, AIAA Paper 2009-5326, Denver, Colorado, August 2009.
- ¹⁸Akiki, M., and Majdalani, J., “Quasi-Analytical Approximation of the Compressible Flow in a Planar Rocket Configuration,” *46th AIAA/ASME/SAE/ASEE Joint Propulsion Conference and Exhibit*, AIAA Paper 2010-7080, Nashville, Tennessee, July 2010.
- ¹⁹Hujeirat, A. A., and Thielemann, F. K., “Numerical Aspects of Low Mach Number Flows in Astrophysics: Preconditioning Techniques,” *Monthly Notices of the Royal Astronomical Society*, Vol. 400, No. 2, December 2009, pp. 903–916. doi:10.1111/j.1365-2966.2009.15498.x.
- ²⁰Nonaka, A., Almgren, A. S., Bell, J. B., Lijewski, M. J., Malone, C. M., and Zingale, M., “Maestro: An Adaptive Low Mach Number Hydrodynamics Algorithm for Stellar Flows,” *Astrophysical Journal Supplement Series*, Vol. 188, No. 2, June 2010, pp. 358–383. doi:10.1088/0067-0049/188/2/358.
- ²¹Hart, R. W., and McClure, F. T., “Combustion Instability: Acoustic Interaction with a Burning Propellant Surface,” *The Journal of Chemical Physics*, Vol. 30, No. 6, 1959, pp. 1501–1514. doi:10.1063/1.1730226.
- ²²Culick, F. E. C., “Rotational Axisymmetric Mean Flow and Damping of Acoustic Waves in a Solid Propellant Rocket,” *AIAA Journal*, Vol. 4, No. 8, 1966, pp. 1462–1464. doi:10.2514/3.3709.
- ²³Fischbach, S., Flandro, G., and Majdalani, J., “Acoustic Streaming in Simplified Liquid Rocket Engines with Transverse Mode Oscillations,” *Physics of Fluids*, Vol. 22, No. 6, 2010, pp. 063602–21. doi:10.1063/1.3407663.
- ²⁴Balakrishnan, G., Lian, A., and Williams, F. A., “Compressible Effects in Thin Channels with Injection,” *AIAA Journal*, Vol. 29, No. 12, 1991, pp. 2149–2154. doi:10.2514/3.11458.
- ²⁵Herczynski, A., and Kasoy, D. R., “Response of a Confined Gas to Volumetric Heating in the Absence of Gravity. 1: Slow Transients,” *Physics of Fluids*, Vol. 3, No. 4, April 1991, pp. 566–577. doi:10.1063/1.858118.
- ²⁶Sirignano, W. A., and Kim, I., “Diffusion Flame in a Two-Dimensional, Accelerating Mixing Layer,” *Physics of Fluids*, Vol. 9, No. 9, September 1997, pp. 2617–2630. doi:10.1063/1.869378.
- ²⁷Shapiro, A. H., *The Dynamics and Thermodynamics of Compressible Fluid Flow*, The Roland Press Company, New York, New York, 1953.
- ²⁸Rayleigh, L., “On the Flow of Compressible Fluid Past an Obstacle,” *Philosophical Magazine*, Vol. 32, No. 1, 1916, pp. 1–6.
- ²⁹Janzen, O., “Beitrag zu einer Theorie der stationären Stromung Kompressibler Flüssigkeiten (Towards a Theory of Stationary Flow of Compressible Fluids),” *Physikalische Zeitschrift*, Vol. 14, 1913, pp. 639–643.
- ³⁰Najjar, F. M., Haselbacher, A., Ferry, J., Wasistho, B., Balachandar, S., and Moser, R., “Large-Scale Multiphase Large-Eddy Simulation of Flows in Solid-Rocket Motors,” *16th AIAA Computational Fluid Dynamics Conference*, AIAA Paper 2003-3700, Orlando, Florida, June 2003.
- ³¹Wasistho, B., Balachandar, S., and Moser, R. D., “Compressible Wall-Injection Flows in Laminar, Transitional, and Turbulent Regimes: Numerical Prediction,” *Journal of Spacecraft and Rockets*, Vol. 41, No. 6, 2004, pp. 915–924. doi:10.2514/1.2019.
- ³²Casalis, G., Avalon, G., and Pineau, J.-P., “Spatial Instability of Planar Channel Flow with Fluid Injection through Porous Walls,” *Physics of Fluids*, Vol. 10, No. 10, 1998, pp. 2558–2568. doi:10.1063/1.869770.
- ³³Griffond, J., “Receptivity and Aeroacoustic Resonance in Channels with Blowing Walls,” *Physics of Fluids*, Vol. 14, No. 11, November 2002, pp. 3946–3962. doi:10.1063/1.1511546.
- ³⁴Maicke, B. A., Saad, T., and Majdalani, J., “On the Compressible Hart-McClure Mean Flow Motion in Simulated Rocket Motors,” *46th AIAA/ASME/SAE/ASEE Joint Propulsion Conference and Exhibit*, AIAA Paper 2010-7077, Nashville, Tennessee, July 2010.
- ³⁵White, F. M., *Fluid Mechanics*, McGraw-Hill, New York, NY, 4th ed., 1999.
- ³⁶Fox, R. W., McDonald, A. T., and Pritchard, P. J., *Introduction to Fluid Mechanics*, John Wiley, New York, NY, 6th ed., 2004.
- ³⁷Taylor, G. I., “Fluid Flow in Regions Bounded by Porous Surfaces,” *Proceedings of the Royal Society of London, Series A*, Vol. 234, No. 1199, March 1956, pp. 456–475. doi:10.1098/rspa.1956.0050.
- ³⁸Gany, A., and Aharon, I., “Internal Ballistics Considerations of Nozzleless Rocket Motors,” *Journal of Propulsion and Power*, Vol. 15, No. 6, November-December 1999, pp. 866–873. doi:10.2514/2.5509.
- ³⁹Hart, R. W., and Cantrell, R. H., “Amplification and Attenuation of Sound by Burning Propellants,” *AIAA Journal*, Vol. 1, No. 2, 1963, pp. 398–404. doi:10.2514/3.1545.
- ⁴⁰Hart, R. W., Bird, J. F., Cantrell, R. H., and McClure, F. T., “Nonlinear Effects in Instability of Solid-Propellant Rocket Motors,” *AIAA Journal*, Vol. 2, No. 7, 1964, pp. 1270–1273. doi:10.2514/3.55069.
- ⁴¹Balakrishnan, G., Lian, A., and Williams, F. A., “Rotational Inviscid Flow in Laterally Burning Solid Propellant Rocket Motors,” *Journal of Propulsion and Power*, Vol. 8, No. 6, 1992, pp. 1167–1176. doi:10.2514/3.10852.